

PIN OR NEEDLE FRAGMENT HR-3031 - TIN BRONZE - LATE BRONZE AGE - SWITZERLAND

Artefact name Pin or needle fragment HR-3031

Authors Marianne. Senn (EMPA, Dübendorf, Zurich, Switzerland) & Christian. Degrigny (HE-Arc CR, Neuchâtel, Neuchâtel, Switzerland)

Url /artefacts/450/

∨ The object



Credit HE-Arc CR.

Fig. 1: Tin bronze pin or needle fragment (after Rychner-Faraggi 1993, plate 74.11),

∨ Description and visual observation

Description of the artefact Pin or needle fragment (Fig. 1). The patina is green-blue and granulated, typical of terrestrial context. Dimensions: L = 9cm; Ø = 2.5-2.9mm; WT = 3.6g.

Type of artefact Pin

Origin Hauterive - Champréveyres, Neuchâtel, Neuchâtel, Switzerland

Recovering date Excavation 1983-1985, object from layer 1 (containing material from the Bronze Age until the 20th century)

Chronology category Late Bronze Age

chronology tpq B.C. ▾

chronology taq B.C. ▾

Chronology comment Hallstatt A2/B

Burial conditions / environment Lake

Artefact location Laténium, Neuchâtel, Neuchâtel

Owner Laténium, Neuchâtel, Neuchâtel

Inv. number Hr 3031

Recorded conservation data Not conserved

Complementary information

Nothing to report.

Study area(s)



Fig. 2: Location of sampling area,

Credit HE-Arc CR.

Binocular observation and representation of the corrosion structure

Stratigraphic representation: none.

MiCorr stratigraphy(ies) – Bi

Sample(s)

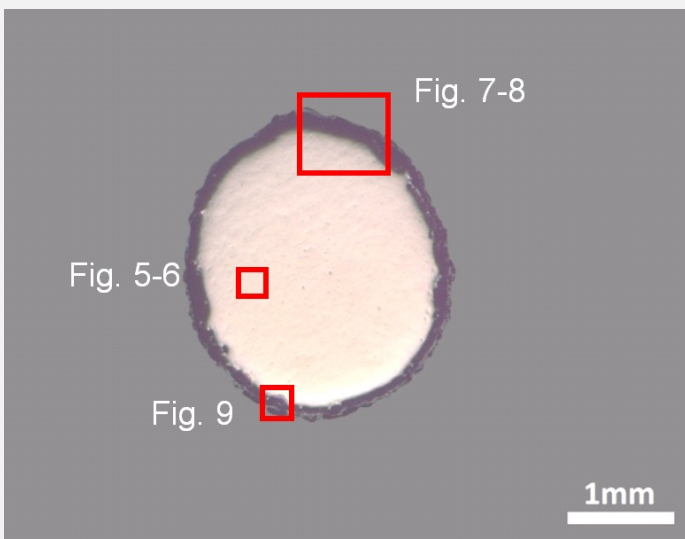


Fig. 3: Micrograph of the cross-section showing the location of Figs. 5 to 9,

Credit HE-Arc CR.

| | |
|---------------------------------|---|
| Description of sample | The cross-section is circular and is a complete section through the pin (Fig. 2). The surface is completely covered with a rather thin corrosion crust of irregular thickness (Fig. 3). |
| Alloy | Tin Bronze |
| Technology | Cold worked after annealing |
| Lab number of sample | MAH 87-195 |
| Sample location | Musées d'art et d'histoire, Genève, Geneva |
| Responsible institution | Musées d'art et d'histoire, Genève, Geneva |
| Date and aim of sampling | 1987, metallography and corrosion characterisation |

Complementary information

Nothing to report.

Analyses and results

Analyses performed:

Metallography (etched with ferric chloride reagent), Vickers hardness testing, ICP-OES, SEM/EDS, XRD.

Non invasive analysis

Metal

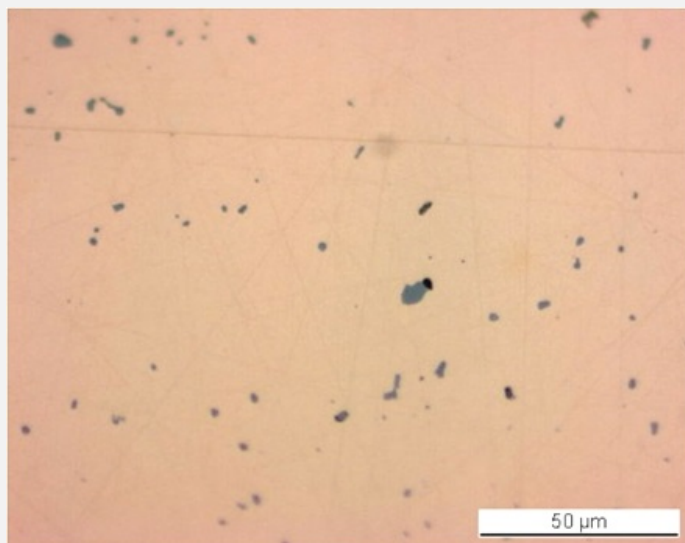
The remaining metal is a tin bronze and contains small copper sulphide and Pb-rich inclusions evenly distributed throughout the metal (Fig. 5, Tables 1 and 2). The Pb-rich inclusions are only visible with SEM appearing as white particles. The etched structure of the tin bronze shows re-crystallised and angular grains, some of them with twins (Fig. 6). Strain or slip lines are visible, especially near the metal surface. They indicate a final cold working. Copper sulphide inclusions are found both at the grain boundaries and inside the grains (Fig. 6). The average hardness of the metal is about HV1 120.

| Elements | Cu | Sn | Sb | Ni | As | Pb | Ag | Co | Zn | Fe |
|----------|-------|------|------|------|------|------|------|------|------|------|
| mass% | 91.29 | 5.65 | 1.00 | 0.69 | 0.55 | 0.51 | 0.22 | 0.06 | 0.01 | 0.02 |

Table 1: Chemical composition of the metal. Method of analysis: ICP-OES, Laboratory of Analytical Chemistry, Empa.

| Elements | S | Cu | Total |
|----------|----|----|-------|
| mass% | 21 | 85 | 106 |

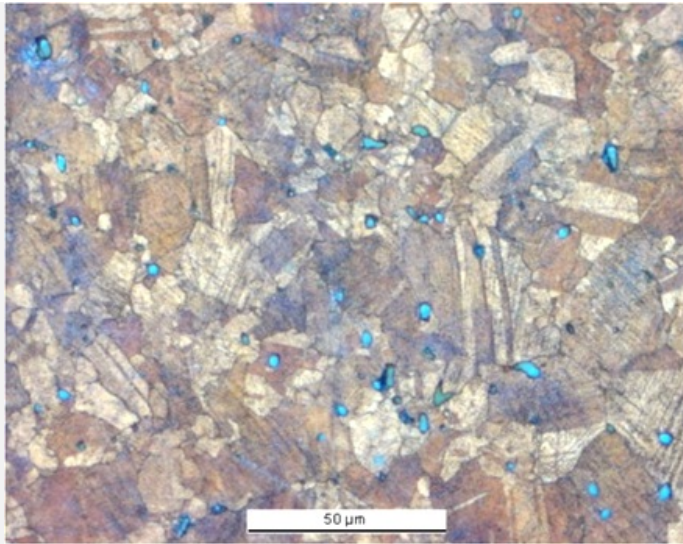
Table 2: Chemical composition of grey inclusions (Fig. 5). Method of analysis: SEM/EDS, Laboratory of Analytical Chemistry, Empa.



Credit HE-Arc CR.

Fig. 5: Micrograph of the metal sample from Fig. 3 (detail), unetched, bright field. Grey copper sulphide inclusions are clearly visible,

Fig. 6: Micrograph of the metal sample from Fig. 3 (detail), etched, bright field. Small angular re-crystallised grains (some with twins)



with slip lines are observed. Copper sulphide inclusions appear in blue,

Credit HE-Arc CR.

| | |
|-----------------------------|---|
| Microstructure | Polygonal and twinned grains + strain lines (metal surface) |
| First metal element | Cu |
| Other metal elements | Ni, As, Ag, Sn, Sb, Pb |

Complementary information

Nothing to report.

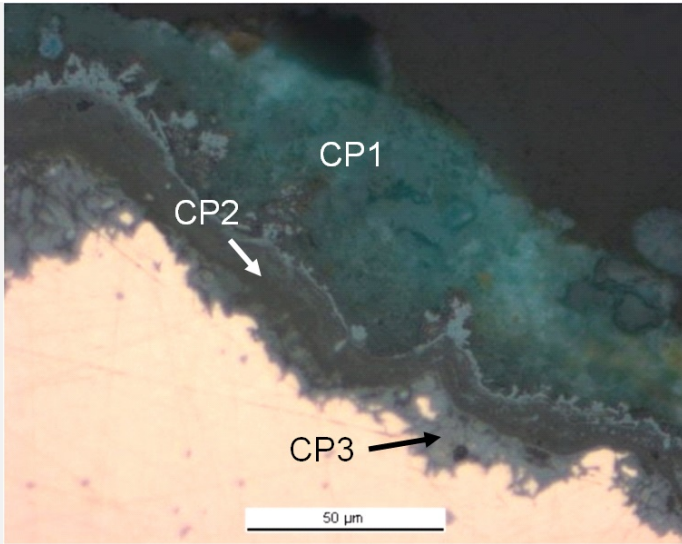
Corrosion layers

The corrosion crust has an average thickness of about 50μm (Fig. 7). In polarised light (Fig. 8), the corrosion stratigraphy is more clearly visible: it is composed of an inner orange-red corrosion layer (CP3, an agglomerate of nanoscale stannic oxides with cuprite) directly on the metal core (Table 3 and Fig. 9, already studied by Piccardo et al. 2007), an intermediate multi-layered black band (CP2) and an outer turquoise-green layer (CP1) analysed with XRD by Schweizer and identified as malachite/CuCO₃Cu(OH)₂ (Schweizer 1994, 150). In some areas the orange-red layers (CP3) can also be found in between the black band (CP2) and the malachite (CP1). Elemental chemical distribution of the SEM image of Fig. 9 shows that the black layers are enriched in Sn but also contain Fe (Fig. 9). Superior markers such as contextual Al and Si are present in the outer malachite layers. S is present both on the rim of the outer black layer and in the malachite (Fig. 9, Table 3).

| Elements | O | Cu | Sn | S | Cl | Fe | As | Ag | Total |
|----------|----|----|----|----|-----|----|-----|-----|-------|
| CP3 ext. | 20 | 40 | 12 | 15 | < | 5 | < | 1.9 | 94 |
| CP3 int. | 20 | 53 | 16 | < | 0.9 | < | 0.6 | < | 91 |

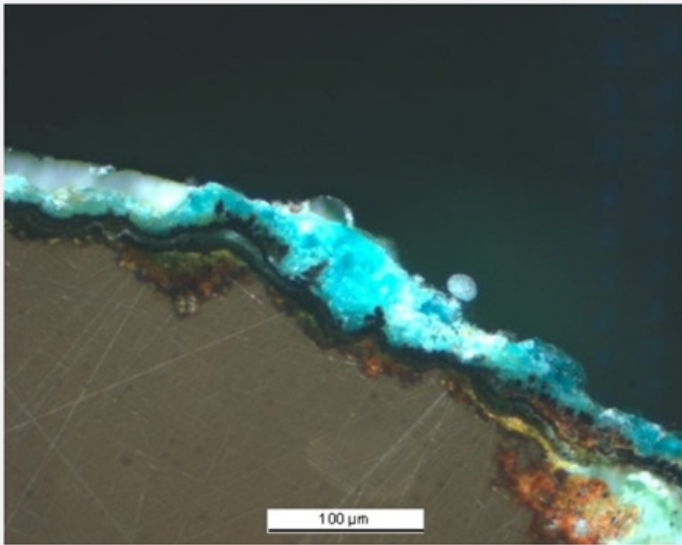
Table 3: Chemical composition (mass %) of orange corrosion products (from Figs. 7 and 8). Method of analysis: SEM/EDS, Laboratory of Analytical Chemistry, Empa.

Fig. 7: Micrograph of the metal sample from Fig. 3 (detail) and corresponding to the stratigraphy of Fig. 4, unetched, bright field. Stratigraphy of the corrosion crust: inner light grey layer (CP3), intermediate dark grey layer with a light-grey rim (CP2) and outer grey-green layer (CP1),



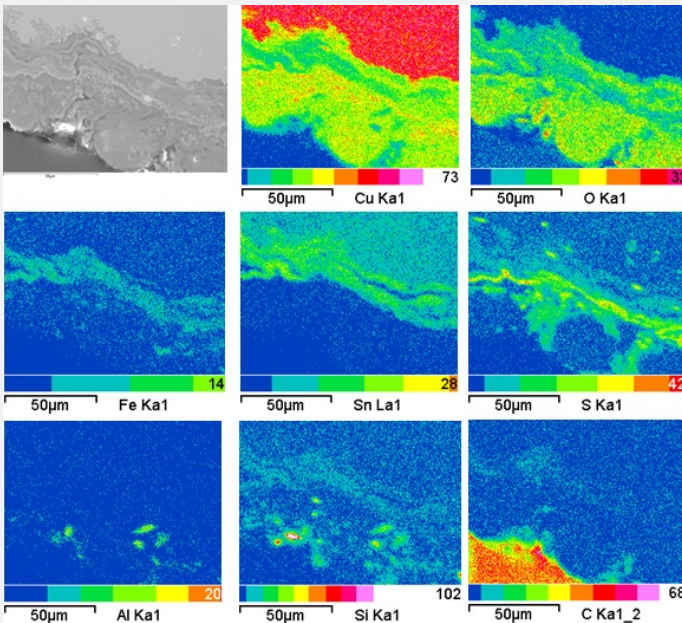
Credit HE-Arc CR.

Fig. 8: Micrograph of the metal sample from Fig. 3 and corresponding to the stratigraphy of Fig. 4, polarised light. The metal appears in brown; the inner layer appears as red-orange, the intermediate layer as black and the outer layer as turquoise,



Credit HE-Arc CR.

Fig. 9: SEM image, SE-mode, and elemental chemical distribution of a selected area of Fig. 3. Method of examination: SEM/EDS, Laboratory of Analytical Chemistry, Empa,



Credit HE-Arc CR.

Corrosion form Multiform - pitting
 Corrosion type Type II (Robbiola)

Complementary information

Nothing to report.

✄ MiCorr stratigraphy(ies) – CS

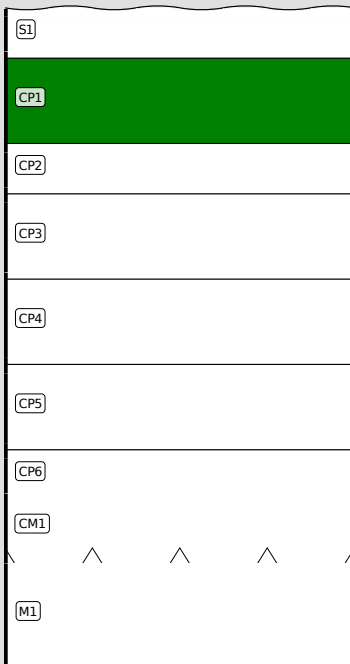


Fig. 4: Stratigraphic representation of the object in cross-section using the MiCorr application. The characteristics of the strata are only accessible by clicking on the drawing that redirects you to the search tool by stratigraphy representation. This representation can be compared to Figs. 7 and 8, Credit HE-Arc CR.

✄ Synthesis of the binocular / cross-section examination of the corrosion structure

Corrected stratigraphic representation: none.

✄ Conclusion

The pin is made from a tin bronze and has been repeatedly cold worked and annealed. After the last annealing there has been some cold work, as can be seen from the strain lines visible after etching the metal. Due to the presence in the corrosion crust of an outer malachite layer, the corrosion was described as terrestrial by Schweizer (Schweizer 1994). The elemental chemical distribution of the corrosion crust shows a more complex situation: as expected for an object buried in a terrestrial site, a typical enrichment of Sn is observed in the inner and intermediate layers covering the remaining metal surface. However it is combined with Fe and S which are often present in lake patinas. According to Schweizer, these layers were formed in anaerobic conditions and developed later on into malachite in an aerated soil through partial dehydration (Schweizer 1994, Schwartz 1934). Since the original surface is absent (destroyed), we refer to type 2 corrosion after Robbiola et al. 1998.

✄ References

References on object and sample

References object

1. Rychner-Faraggi A-M. (1993) Hauterive – Champréveyres 9. Métal et parure au Bronze final. Archéologie neuchâteloise, 17 (Neuchâtel), planche 74.11.

References sample

2. Empa Report 137 695/1991, P.O. Boll.
3. Rapport d'examen, Laboratoire Musées d'art et d'Histoire, Geneva GE (1987), 87-194 à 197.
4. Schwartz, G.M. (1934) Paragenesis of oxidised ores of copper, *Economic Geology*, 29, 55-75.
5. Schweizer, F. (1994) Objets en bronze provenant de sites lacustres: de leur patine à leur biographie. In: *L'œuvre d'art sous le regard des sciences* (éd. Rinuy, A. and Schweizer, F.), 143-157.

References on analytic methods and interpretation

6. Interpretation of orange corrosion products, see: Piccardo P., Mille B., Robbiola L. Tin and copper oxide in corroded archaeological bronzes, In: *Corrosion of metallic heritage artefacts*, European Federation of Corrosion Publication n°48, 2007, ed. Dillmann et al, 239-262.
7. Robbiola, L., Blengino, J-M., Fiaud, C. (1998) Morphology and mechanisms of formation of natural patinas on archaeological Cu-Sn alloys, *Corrosion Science*, 40, 12, 2083-2111.